

# Interface between light coupled to excited-states transition and ground-state coherence of rubidium atoms

Michał Parniak, Adam Leszczyński, and Wojciech Wasilewski  
*Institute of Experimental Physics, Faculty of Physics,  
 University of Warsaw, Pasteura 5, 02-093 Warsaw, Poland*

We demonstrate an interface between light coupled to transition between excited states of rubidium and long-lived ground-state atomic coherence. In our proof-of-principle experiment a non-linear process of four-wave mixing in an open-loop configuration is used to achieve light emission proportional to independently prepared ground-state atomic coherence. We demonstrate strong correlations between Raman light heralding generation of ground-state coherence and the new four-wave mixing signal. Dependence of the efficiency of the process on laser detunings is studied.

Off-resonant Raman scattering is a robust approach to light-atom interfaces. One of the methods is to induce spontaneous Stokes scattering in which pairs of photons and collective atomic excitations - a two-mode squeezed state - are created. These excitations can be stored and later retrieved in the anti-Stokes process [1]. This approach is commonly known to be a basic building block of the DLCZ protocol [2].

Typically rubidium and cesium have been used as atomic systems in both warm and cold atomic ensembles [3–5]. These systems are coupled to light at near-IR wavelengths, such as 795 and 780 nm for rubidium D1 and D2 lines. To extend possibilities of quantum memories, coupling to new wavelengths is required. This can be accomplished by non-linear frequency conversion in the four-wave mixing (4WM) process using strong resonant non-linearities in atoms thanks to transitions between excited states. The diamond configuration has been used to demonstrate frequency conversion in rubidium [6–9]. The same configuration has been used to generate photon pairs in the cascaded spontaneous 4WM process [10, 11]. Multiphoton processes are also a developing method to interface light and Rydberg atoms [12, 13].

Chanelière et al. [14] proposed to combine the processes of Raman scattering and 4WM by first creating photon pairs in a cascaded spontaneous 4WM in one atomic ensemble and then storing photons as collective atomic excitations in another cold ensemble, and an experiment was recently realized by Zhang et al. [15]. As a result they obtained a two-mode squeezed state of atomic excitations and telecom photons. Another approach was to frequency-convert light generated in quantum memory with 4WM, which was realized by Radnaev et al. [16], in order to create a frequency-converted quantum memory. In all cases one atomic ensemble was used for storage, and another for frequency conversion or photon generation.

In this Letter we propose and realize a Raman-like interface based on 4WM in warm rubidium vapors. The process we present may be in principle used to generate correlated pairs of collective atomic excitations and photons coupled to transition between two excited states in a single, four-photon process in a single atomic ensemble. We use  $5P_{3/2}$  and  $5D_{5/2}$  as intermediate states in the process. Transition between two excited states corresponds

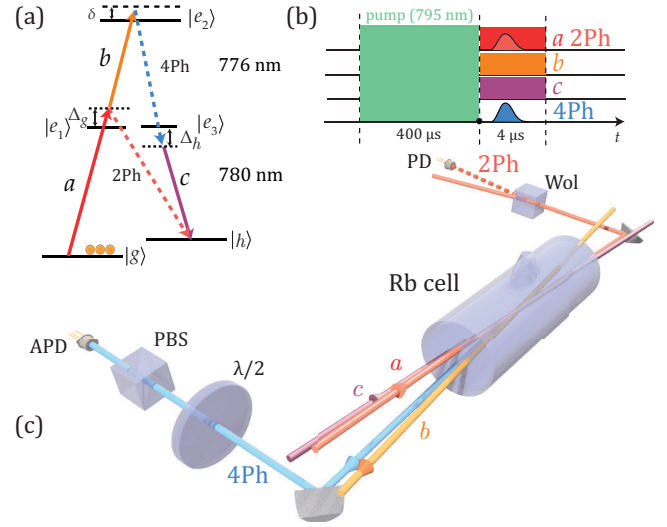


FIG. 1. (a) Configuration of atomic levels and fields we use to realize the four-photon interface, (b) pulse sequence used in the experiment and (c) the central part of experimental setup demonstrating phase-matching geometry. Rows in (b) correspond to different beam paths presented in (c).

to 776-nm light as illustrated in Fig. 1(a).

In our experiment we generate ground-state atomic coherence  $\rho_{gh}$  and light denoted by 2Ph in a two-photon process [17, 18]. We observe concurrent generation of 776-nm light denoted by 4Ph in a four-photon process analogous to stimulated Raman scattering driven by ground-state coherence. It does not occur spontaneously in the macroscopic regime due to small gain. However, with macroscopic  $\rho_{gh}$  the driving fields  $a$ ,  $b$  and  $c$  couple ground-state atomic coherence to the weak optical 4Ph field. In the leading order in drive beam fields Rabi frequencies  $\Omega_i$  the atomic polarization resulting in emission of 4Ph signal field is:

$$\mathbf{P} = -2n\mathbf{d}_{e_3e_2}\rho_{gh}\frac{\Omega_a\Omega_b\Omega_c^*}{8\Delta_g\delta\Delta_h}, \quad (1)$$

where  $n$  is the atom number density and  $\mathbf{d}_{ij}$  is the

dipole moments of respective transition. From this formula it follows which detunings play role.

For the experimental observation a prior knowledge of polarization properties is crucial. To find it, one has to add contributions from all possible paths through intermediate hyperfine states. Since the detunings from intermediate  $5P_{3/2}$  state are much larger than respective hyperfine splittings we ignored the latter. Same approximation has been adopted for the highest excited state  $5D_{5/2}$ . Even though respective detuning  $\delta$  it is of the order of several MHz, similar to the hyperfine splitting of the highest excited state  $5D_{5/2}$ , the hyperfine structure is completely unresolved due to significant pressure broadening [19] in 5 torr neon as buffer gas we use. Consequently, we may omit any detuning dependance and calculate the unnormalized polarization vector  $\epsilon$  of the signal light using path-averaging formalism we developed in [8], by decalling the definitions of Rabi frequencies in Eq. (1):

$$\epsilon = \sum_{F, m_F} \mathbf{d}_{e_3 e_2} (\mathbf{E}_a \cdot \mathbf{d}_{g e_1} \mathbf{E}_b \cdot \mathbf{d}_{e_1 e_2} \mathbf{E}_c^* \cdot \mathbf{d}_{e_3 h}^*), \quad (2)$$

where  $\mathbf{E}_i$  are electric fields of respective beams  $i$ . Summation is carried over all possible magnetic sublevels ( $F_i$ ,  $m_{F_i}$ ) of all intermediate states  $|e_1\rangle$ ,  $|e_2\rangle$  and  $|e_3\rangle$ .

The experimental setup is build around the rubidium-87 vapor cell heated to  $100^\circ\text{C}$ . For the two lowest, long-lived states, we use two hyperfine components of rubidium ground-state manifold, namely  $|5S_{1/2}, F=1\rangle = |g\rangle$  and  $|5S_{1/2}, F=2\rangle = |h\rangle$ . For the  $|e_1\rangle$  and  $|e_3\rangle$  states we take hyperfine components of the  $5P_{3/2}$  manifold, and for the highest excited state  $|e_2\rangle$  we take the  $5D_{5/2}$  manifold. Atoms are initially pumped into  $|g\rangle$  state using  $400 \mu\text{s}$  optical pumping pulse. Next, three driving pulses of  $4 \mu\text{s}$  duration each are applied simultaneously, as shown in Fig. 1(b). Inside the cell, beams are collimated and have diameters of  $400 \mu\text{m}$ , being well-overlapped over a 2-cm-long cylindrical region. They intersect at a small angle of  $14 \text{ mrad}$ , with 780-nm beams nearly counter-propagating with respect to the 776-nm beams, as presented in Fig. 1(c). Powers of driving beams  $a$ ,  $b$  and  $c$  are 10 mW, 45 mW and 8 mW, respectively.

The 780-nm two-photon Raman signal 2Ph co-propagates with the driving field  $a$ . It is separated using a Wollaston polarizer (Wol) and detected on a fast photodiode (PD). The four-photon signal 4Ph, is emitted in the direction given by the phase matching condition  $\mathbf{k}_a + \mathbf{k}_b = \mathbf{k}_{4\text{Ph}} + \mathbf{k}_c$ . In addition to the desired 4Ph signal, 776-nm light coming from the closed-loop process in which field  $c$  couples level  $|e_3\rangle$  directly to  $|g\rangle$  is emitted in the same direction [8] and at a frequency differing by only 6.8 GHz. However, when driving fields  $a$ ,  $b$  and  $c$  are  $x$ -,  $y$ - and  $y$ - polarized, respectively, the 4Ph signal light is  $x$ -polarized, while the closed-loop 4WM light is  $y$ -polarized, where  $x \perp y$ . This arrangement enables filtering out the 4Ph signal from both stray 776-nm driving light and the closed-loop 4WM light with a polariz-

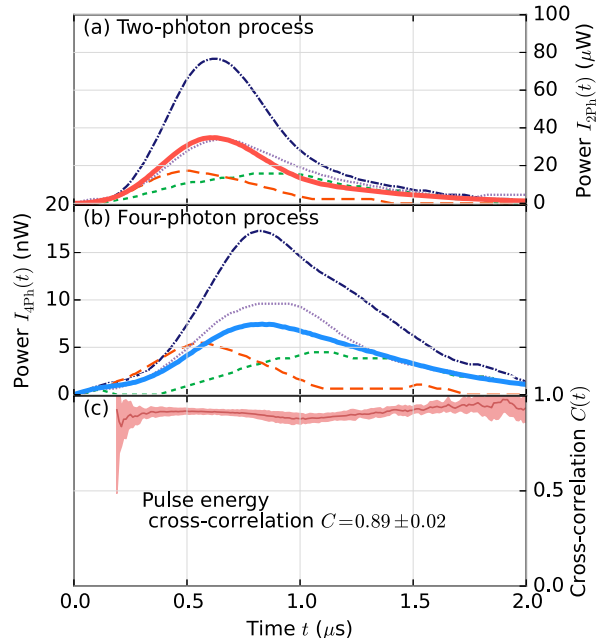


FIG. 2. (a - 2Ph, b - 4Ph) Averaged signal intensities (solid lines) with several single realizations (dashed lines), denoted by same colors in (b) and (c), demonstrating visible strong correlations and (c) calculated cross-correlation  $C(t)$  between signals of four-photon (4Ph) and the two-photon processes (2Ph).

ing beam-splitter (PBS). To suppress residual drive laser background 4Ph signal goes through an interference filter and is detected by an avalanche photodiode (APD). We verified the frequencies of 4Ph and closed loop light using a scanning Fabry-Perot confocal interferometer. By rotating the half-wave plate ( $\lambda/2$ ) we could easily switch between observing 4Ph and closed loop signal. They display different temporal characteristics, also only 4Ph is correlated with the 2Ph light.

In our experiment we remain in the macroscopic scattered light intensity regime. When strong Raman driving field is present, atoms are transferred to  $|h\rangle$  in large numbers simultaneously with scattering of 2Ph photons and buildup of large atomic coherence  $\rho_{gh}$  [17]. The temporal shape of the 2Ph pulse is an exponential only at the very beginning, which we observe in Fig. 2(a). The pulse shapes fluctuate significantly from shot to shot, as the process is seeded by vacuum fluctuations [3]. However, the 4Ph pulse, presented in Fig. 2(b), nearly exactly follows the 2Ph pulse. We calculated temporal correlations between the 2Ph signal, which is known to be proportional to the ground-state atomic coherence  $\rho_{gh}$ , and the 4Ph signal. Normalized intensity correlation at time  $t$  between the 2Ph signal  $I_{2\text{Ph}}(t)$  and the 4Ph signal  $I_{4\text{Ph}}(t)$  were calculated according to the formula  $C(t) = \langle \Delta I_{2\text{Ph}}(t) \Delta I_{4\text{Ph}}(t) \rangle / \sqrt{\langle \Delta I_{2\text{Ph}}^2(t) \rangle \langle \Delta I_{4\text{Ph}}^2(t) \rangle}$  by

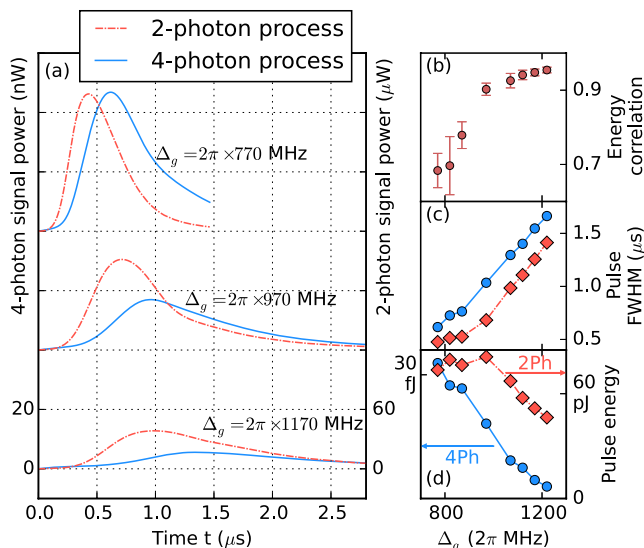


FIG. 3. Temporal profiles of the studied processes: (a) averaged pulse shapes for the intensities of the 2Ph and the 4Ph for a set of single-photon detunings  $\Delta_g$  for a constant two-photon detuning  $\delta/2\pi = -50$  MHz, (b) pulse energy correlation between the two processes as, (c) pulses full-width at half-maxima (FWHM) and (d) their energies as a function of field  $a$  single photon detuning  $\Delta_g$ . Subsequent plots of 2Ph (4Ph) signals in (a) are shifted by 120  $\mu$ W (40 nW).

averaging over 500 realizations, where the standard deviations  $\langle \Delta I_{2\text{Ph}}^2(t) \rangle$  and  $\langle \Delta I_{4\text{Ph}}^2(t) \rangle$  are corrected for electronic noise. Figure 2(c) presents the cross-correlation  $C(t)$ . We observe that correlations are high during the entire process, which proves that at any time both processes interact with the same atomic coherence  $\rho_{gh}$  [20]. In particular, we were able to measure high correlation at the very beginning of the pulses, where light intensities are low. This regime is quite promising for further quantum applications. To estimate the uncertainty of calculated correlations, we divided data into 10 equal sets of 50 repetitions and calculated the correlation inside each set to finally obtain estimate of uncertainty by calculating standard deviation of results from all repetitions.

Now we switch to verifying properties of 4Ph signal for various drive field detunings. The influence of field  $a$  detuning  $\Delta_g$  is seen in Fig. 3. A number of pronounced effects come about as this laser drives the Raman scattering and produces ground-state atomic coherence  $\rho_{gh}$ . In turn  $|\rho_{gh}|^2$  is proportional to the intensity of 2Ph light for off-resonant drive field. Initially the 2Ph signal grows exponentially and the corresponding Raman gain coefficient is strongly dependent on drive field detuning  $\Delta_g$ . Strong Raman driving field transfers atoms to  $|h\rangle$  in large numbers resulting in gain saturation. The 4Ph pulse follows the ground-state atomic coherence  $\rho_{gh}$  and 2Ph pulse as shown in the previous section, however its maximum is somewhat delayed. We attribute this effect to internal atom dynamics at high drive intensity levels which is not captured by Eq. (1). Energies of pulses are

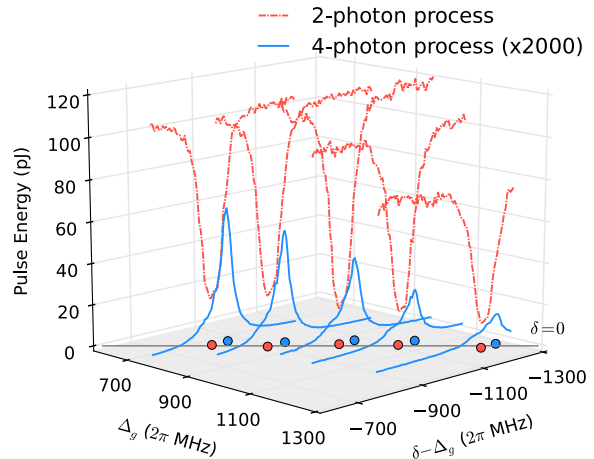


FIG. 4. Experimental average pulse energies of 2Ph and 4Ph signals as a function of field  $a$  detuning  $\Delta_g$  (measured from  $F = 1 \rightarrow F' = 1$  resonance) and field  $b$  detuning  $\delta - \Delta_g$  around the two-photon resonance. As we change the field  $a$  detuning both single photon detuning  $\Delta_g$  and the two-photon detuning  $\delta$  change accordingly. Dots represent maxima (minima) of the 4Ph (2Ph) signal.

also higher closer to resonance, although the two-photon Raman pulse energy saturates due to absorption losses.

Important insight is provided by calculating energy correlation between the 2Ph and 4Ph light pulses, which fluctuate significantly from shot to shot. Correlation is calculated as  $C = \langle \Delta E_{2\text{Ph}} \Delta E_{4\text{Ph}} \rangle / \sqrt{\langle \Delta E_{2\text{Ph}}^2 \rangle \langle \Delta E_{4\text{Ph}}^2 \rangle}$ , where  $E_{2\text{Ph}}$  and  $E_{4\text{Ph}}$  are total energies of 2Ph and 4Ph light pulses, respectively, in a single realization. The averaging  $\langle \cdot \rangle$  is done over 500 realizations of the process and results are plotted in Fig. 3(b). Strong correlations reinforce the observation that indeed we are able to couple 4Ph optical field to the ground-state coherence, since number of photons in the 2Ph pulse is proportional to generated atomic coherence  $|\rho_{gh}|^2$ . We attribute the drop in correlations close to resonance line to absorption losses.

To capture the physics in the vicinity of the two-photon resonance we studied 4Ph and 2Ph pulse energies as a function of detunings of fields  $a$  and  $b$ . First we scan the field  $b$  detuning  $\delta - \Delta_g$  across the two-photon resonance line (see Fig. 4). We observed strong suppression of 2Ph signal due to two-photon absorption (TPA) in ladder configuration [21]. As a consequence, less atomic coherence  $\rho_{gh}$  is generated and the 4Ph signal is also reduced. In turn, the 4Ph signal intensity is a trade-off between TPA losses and 4WM efficiency, as the latter is highest at the two-photon resonance according to Eq. (1). This behavior is typical for off-resonant Raman scattering interfaces. By changing the field  $a$  detuning  $\Delta_g$  we observed expected shifting of the two-photon resonance.

Contrary to the above, changing the detuning  $\Delta_h$  of

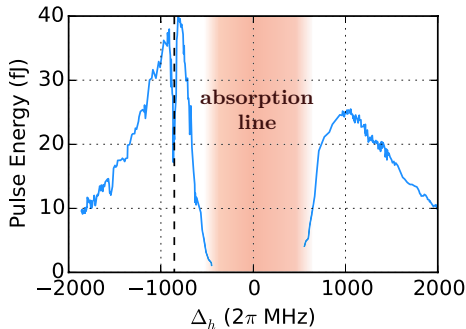


FIG. 5. Four-photon signal pulse energy as a function of the detuning  $\Delta_h$  (measured from  $F = 2 \rightarrow F' = 2$  resonance) of field  $c$  for optimal conditions of other lasers ( $\Delta_g/2\pi = 900$  MHz and  $\delta/2\pi = -50$  MHz). Absorption line corresponds to the  $F = 2$  hyperfine component of the ground state, where the right side of the plot is the red-detuned side. Drop at around  $\Delta_h/2\pi = -900$  MHz corresponds exactly to  $6.8 \times 2\pi$  GHz detuning between the two 780-nm lasers, or  $\Delta_g + \Delta_h = 0$ .

the 780-nm driving field  $c$  has only mild effect on the 4Ph signal. Fig. 5 presents 4Ph signal pulse energy as a function of  $\Delta_h$  while other lasers were tuned for maximal signal ( $\Delta_g/2\pi = 900$  MHz and  $\delta/2\pi = -50$  MHz). Since the 4Ph field frequency adapts to match the energy conservation for the  $|h\rangle \rightarrow |e_3\rangle \rightarrow |e_2\rangle$  two-photon transition, the frequency of the driving field  $c$  is not critical. The laser must only be off-resonant, so the driving field is not absorbed and does not disturb the ground-state coherence. We also observed a marked narrow drop in 4Ph process efficiency when the detuning between fields  $a$  and  $c$  is exactly the ground-state hyperfine splitting, or equivalently  $\Delta_g + \Delta_h = 0$ , which is due to  $\Lambda$  configuration two-photon resonance yielding strong interaction with the ground-state coherence.

In conclusion, the experiment we performed is a proof-of-principle of a new light atom interface that enables coupling of long-lived ground-state atomic coherence and light resonant with transition between excited states. The non-linear process we discussed is a novel type of process with typical characteristics of both Raman scattering and 4WM. We generated ground-state atomic coherence via the well known two-photon process. We demonstrated that we are able to couple the very same atomic coherence to optical field resonant with transition between two excited states via a four-photon process. This was verified by measuring high correlations between 2Ph and 4Ph fields, as well as frequency and polarization char-

acteristics of the four-photon process.

We studied the behavior of pulse shapes as a function of driving laser detunings. Among many results, we found that maximum signal is achieved when lasers are detuned from the two-photon resonance by approximately  $\delta = -50 \times 2\pi$  MHz, which is a trade-off between TPA spoiling the generation of atomic coherence, and the efficiency of the four-photon process. This results demonstrate that we are able to control the 4WM process with ground-state coherence, which constitutes a novel type of Raman scattering driven by three non-degenerate fields, in analogy to hyper-Raman scattering where the scattering process is driven by two degenerate fields.

In our experiment we used light at 776 nm coupled to  $5P_{3/2} \rightarrow 5D_{5/2}$  transition. Using different states, such as  $4D_{3/2}$  as the highest excited state, and  $5P_{1/2}$  and  $5P_{3/2}$  as two intermediate states, would enable coupling telecom light (namely at 1475.7 nm or 1529.3 nm). We envisage using such process as a building block for a telecom quantum repeater or a quantum memory. By applying external weak quantum field as the 4Ph field, the system may serve as an atomic quantum memory, based on a highly non-linear process as in [22], but still linear in the input field amplitude. It may also solve many problems with filtering [23], since many similar configurations exists (e.g. with  $5P_{3/2}$ ,  $5D_{3/2}$  and  $5P_{1/2}$  as intermediate states) in which all driving lasers operate at different wavelengths than the signal. We believe such a process might also be used as a non-linear spectroscopy method. Additionally, 4WM character of the process enables engineering of phase-matching condition, namely changing angles between incident driving beams to change spatial patterns of ground-state coherence, known as spin-waves [3], to explore spatially-multimode capabilities of the system. In future studies of the process we propose to address patterns unachievable by typical Raman light-atom interface based on  $\Lambda$  level configuration. Pulse temporal profiles should also be further investigated [24], as they may enable interesting hamiltonian engineering [5]. As a final remark we note that using a cold atomic ensemble would offer selectivity in intermediate states of the process and small detunings, thus enabling better polarization control and efficiency of the process.

*Funding.* Polish Ministry of Science and Higher Education “Diamentowy Grant” Project No. DI2013 011943 and National Science Center (Poland) Grant No. 2011/03/D/ST2/01941.

*Acknowledgment.* We acknowledge insightful discussions with R. Chrapkiewicz, M. Dąbrowski and J. Nunn as well as generous support of K. Banaszek and T. Stacewicz.

[1] C. H. van der Wal, M. D. Eisaman, A. André, R. L. Walsworth, D. F. Phillips, A. S. Zibrov, and M. D. Lukin, *Science* **301**, 196 (2003).

[2] L. M. Duan, M. D. Lukin, J. I. Cirac, and P. Zoller, *Nature* **414**, 413 (2001).

- [3] R. Chrapkiewicz and W. Wasilewski, *Optics Express* **20**, 29540 (2012).
- [4] P. S. Michelberger, T. F. M. Champion, M. R. Sprague, K. T. Kaczmarek, M. Barbieri, X. M. Jin, D. G. England, W. S. Kolthammer, D. J. Saunders, J. Nunn, and I. A. Walmsley, *New Journal of Physics* **17**, 043006 (2015).
- [5] M. Dąbrowski, R. Chrapkiewicz, and W. Wasilewski, *Optics Express* **22**, 26076 (2014).
- [6] P. S. Donvankar, V. Venkataraman, S. Clemmen, K. Saha, and A. L. Gaeta, *Optics Letters* **39**, 1557 (2014).
- [7] F. E. Becerra, R. T. Willis, S. L. Rolston, and L. A. Orozco, *Physical Review A* **78**, 013834 (2008).
- [8] M. Parniak and W. Wasilewski, *Physical Review A* **91**, 023418 (2015).
- [9] A. A. M. Akulshin, R. J. R. McLean, A. I. Sidorov, and P. Hannaford, *Optics Express* **17**, 22861 (2009).
- [10] R. T. Willis, F. E. Becerra, L. A. Orozco, and S. L. Rolston, *Physical Review A* **82**, 053842 (2010).
- [11] B. Srivathsan, G. K. Gulati, B. Chng, G. Maslennikov, D. Matsukevich, and C. Kurtsiefer, *Physical Review Letters* **111**, 123602 (2013).
- [12] J. M. Kondo, N. Šibalić, A. Guttridge, C. G. Wade, N. R. De Melo, C. S. Adams, and K. J. Weatherill, *Optics Letters* **40**, 5570 (2015).
- [13] B. Huber, A. Kölle, and T. Pfau, *Physical Review A* **90**, 053806 (2014).
- [14] T. Chanelière, D. Matsukevich, S. Jenkins, T. Kennedy, M. Chapman, and A. Kuzmich, *Physical Review Letters* **96**, 093604 (2006).
- [15] W. Zhang, D.-S. Ding, S. Shi, Y. Li, Z.-Y. Zhou, B.-S. Shi, and G.-C. Guo, arXiv:1508.07754 (2015).
- [16] A. G. Radnaev, Y. O. Dudin, R. Zhao, H. H. Jen, S. D. Jenkins, A. Kuzmich, and T. A. B. Kennedy, *Nature Physics* **6**, 894 (2010).
- [17] K. Zhang, J. Guo, C.-H. Yuan, L. Q. Chen, C. Bian, B. Chen, Z. Y. Ou, and W. Zhang, *Physical Review A* **89**, 063826 (2014).
- [18] C.-H. Yuan, L. Q. Chen, J. Jing, Z. Y. Ou, and W. Zhang, *Physical Review A* **82**, 1 (2010).
- [19] N. D. Zamoski, G. D. Hager, C. J. Erickson, and J. H. Burke, *Journal of Physics B: Atomic, Molecular and Optical Physics* **47**, 225205 (2014).
- [20] L. Q. Chen, G.-W. Zhang, C.-L. Bian, C.-H. Yuan, Z. Y. Ou, and W. Zhang, *Physical Review Letters* **105**, 133603 (2010).
- [21] H. S. Moon and H.-R. Noh, *Optics Express* **21**, 7447 (2013).
- [22] R. A. de Oliveira, G. C. Borba, W. S. Martins, S. Barreiro, D. Felinto, and J. W. R. Tabosa, *Optics Letters* **40**, 4939 (2015).
- [23] M. Dąbrowski, R. Chrapkiewicz, and W. Wasilewski, *Journal of Modern Optics* (2015).
- [24] A. Raczyński, J. Zaremba, and S. Zielińska-Raczyńska, *Journal of the Optical Society of America B* **32**, 1229 (2015).